The Visual Computer

3D Visualization of tomographic volume data using the generalized voxel model*

Karl Heinz Höhne,
Michael Bomans,
Andreas Pommert, Martin Riemer,
Carsten Schiers, Ulf Tiede,
and Gunnar Wiebecke

Institute of Mathematics and Computer Science
in Medicine, University Hospital Eppendorf,
D-2000 Hamburg, Federal Republic of Germany

Multi-slice images obtained from computer tomography and magnetic resonance imaging represent a 3D image volume. For its visualization we use a ray-casting algorithm working on a gray-scale voxel data model. This model is extended by additional attributes such as membership to an organ or a second imaging modality ("generalized voxel model"). It is shown that the combination of different surface-rendering algorithms together with cutting and transparent display allow a realistic visualization of the human anatomy.

Key words: Computer tomography – Magnetic resonance imaging – Ray-casting algorithm – Voxel

* The investigations were supported in part by the Deutsche Forschungsgemeinschaft and the Werner Otto Foundation, Hamburg

1 Introduction

Ever-increasing numbers of medical diagnostic images are obtained from X-ray computed tomography (CT), magnetic resonance imaging (MRI), and positron emission tomography (PET), which produce sequences of 2D cross-sectional slices. The most usual method of analyzing these images at present is sequential observation of individual 2D slices and the viewer's subsequent "mental reconstruction" of the 3D relationships. Computerized reconstructions of CT scans have produced 3D perspective displays of bone anatomy that have proven clinically useful in craniofacial surgery and orthopedics (Hemmy et al. 1983; Templeton et al. 1984; Vannier et al. 1984; Yasuda et al. 1984; Boecker et al. 1985; Chen et al. 1985; Herman et al. 1985; Witte et al. 1986). The procedures used in these applications are limited by the fact that only pre-defined surfaces (mostly bone) can be visualized and that all other information is not used or is lost during processing. A few recent investigations have dealt with the software and hardware problems of displaying 3D tomographic volumes that preserve the entire original gray-scale data, thus allowing a detailed exploration of the volume (Goldwasser et al. 1985; Jackel 1985; Lenz et al. 1986; Kaufman 1986; Höhne et al. 1987). On the basis of data from CT and MRI we have developed, investigated and compared a variety of methods for visualizing gray-level volumes.

2 Method and results

2.1 Data structure

The raw data consist of a spatial sequence of image matrices of 256^3 or 512^3 pixels. To save storage space, the gray-level data of the original volume is compressed to a dynamic range of 256 gray values. To achieve cubic volume elements, a linear interpolation of the intensity values between the original slices is performed. The 3D array obtained in this manner ("voxel model") is the basic data structure for most of the algorithms described (see Fig. 1). As an extension, each voxel may contain not only a gray value but also further attributes, such as membership to an organ or an intensity value delivered by an additional imaging modality ("generalized voxel model"). In the present implementation each voxel is defined by up to 16 bits.

The Visual Computer (1990) 6:28–36

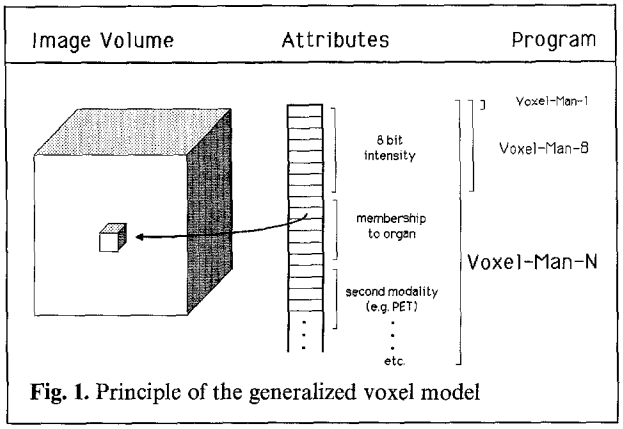

Fig. 1. Principle of the generalized voxel model

2.2 Projection strategy

When scanning the volume we basically have the choice between two classes of strategies: one class consists of the object-space oriented methods that scan along lines or columns of the 3D array and project a chosen aspect onto an image plane in the direction of view. These are known as back-to-front (BTF) of front-to-back (FTB) methods. They have proven to be reasonably fast when a pure surface display of a single object is required. When, however, volumetric properties such as translucency are to be visualized, image-space oriented methods that scan the image volume along the viewing direction are unavoidable. The computing overhead of this algorithm, referred to as ray casting (see Fig. 2), is larger, especially when the whole data volume does not fit into the main memory of the hardware. Therefore, in our project we use a FTB algorithm for the visualization of pure surfaces. For all other projections we rotate the whole volume so that scanning for a desired viewing direction can be done along the lines of the array. Thus, the time-consuming coordinate transformation has to be performed only once per viewing direction. The gray-level assignment in the rotated volume is done by trilinear interpolation. Optionally, the volume can be distorted so that a central projection is achieved. All pictures in this article have been produced in this way.

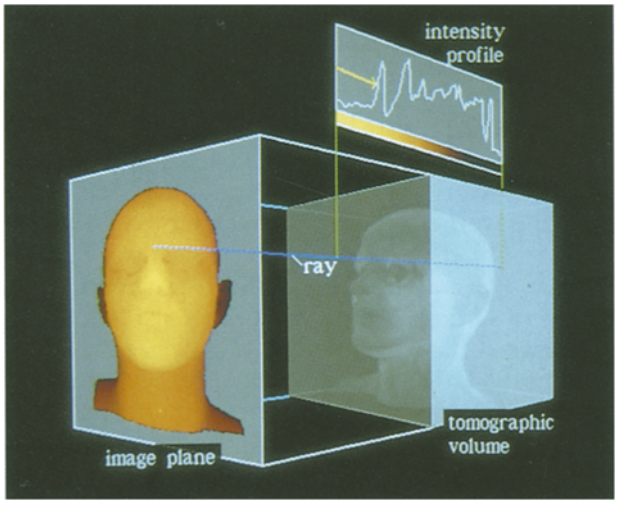

Fig. 2. Principle of the ray-casting algorithm. A parameter obtained from the intensity profile along the ray is projected to an image plane

2.3 Surface rendering

The classic approach to visualization of a volume is the display of surfaces contained in it. The easiest way of determining the voxels that represent a surface (segmentation) is intensity thresholding. This works quite well for the outer skin in MRI and CT as well as for bone in CT. As is well-known, a raw image of the surface determined using this method can be produced by imaging the negative distance to the observer (Z-buffer (Z) shading, see Fig. 3a). Naturally, for realistic images, the surface-normal vectors have to be determined. A method that is not too time-consuming is the estimation of the surface normals from the Z-buffer (Chen et al. 1985), in our project further referred to as Z-buffer gradient (ZG) shading. We have implemented a modified version of this algorithm (Tiede et al. 1987). This algorithm delivers fairly realistic images, but it suffers from the fact that the dynamic range of surface angles is low (Fig. 3b). This is because they are computed on the basis of the position of surface voxels in a 3×3 neighborhood that does not allow a large number of choices.

Much better results can be obtained if the gray-scale data are utilized for the determination of the surface normals. As a consequence of the tomographic data acquisition technique, the gray values in the neighborhood of a surface voxel reflect the relative average of the various tissue types (usually two: air/skin and soft tissue/bone) in the voxels immediately adjacent to the voxel in question. These relative volumes are related to the surface inclination. Thus, the gray-level gradient can be considered a measure for surface inclination. This idea of gray-level gradient (GG) shading has been described by Barillot et al. (1985) and independent-

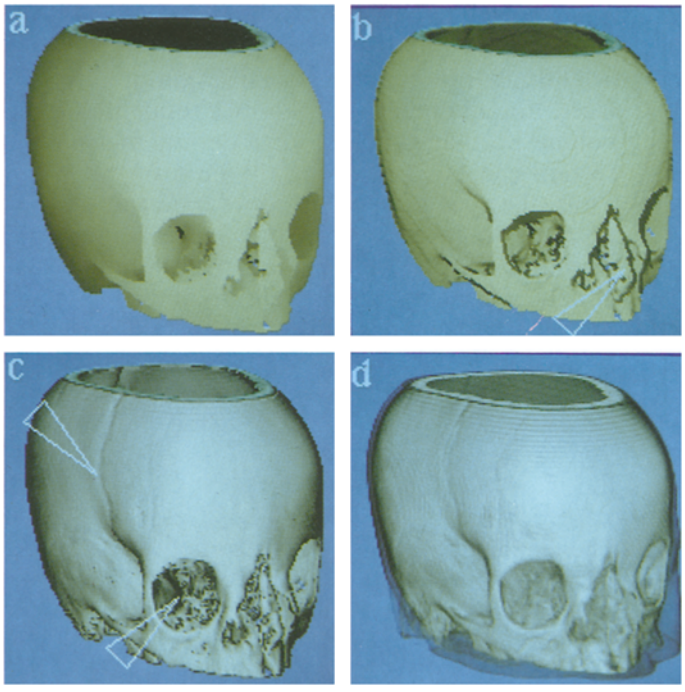

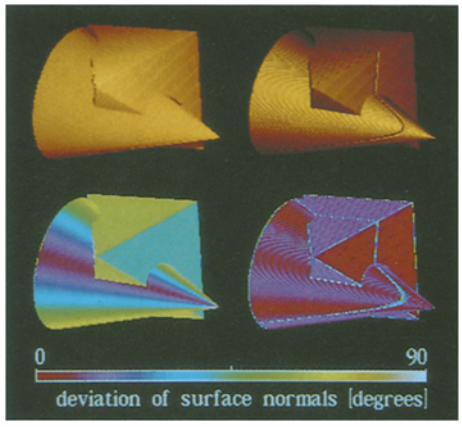

Fig. 4. Comparison of shading methods using an artificial object consisting of a cone and a pyramid with a slit.
Upper left: Z-buffer gradient shading.
Upper right: gray-level gradient shading. The error images (*bottom*) demonstrate the deviation of the computed surface normals from reality

Fig. 3a–d. Skull of a child with a facial cleft reconstructed from 61 computer tomograms using: **a** Z-buffer shading, **b** Z-buffer gradient shading (*arrow* points to the deformed nasal septum), **c** gray-level gradient shading (*arrows* point to a suture and the orbital cavity, respectively), **d** transparent gray-level gradient shading

ly by Höhne and Bernstein (1986) and Tiede et al. (1987, 1988). The algorithm published by Lorensen et al. (1987) functions on the same basis. Our procedure is as follows:
Given the gray level of a surface voxel at a location i, j, k, the gray level gradient is computed as:

$$G_x = g_{(i+1,j,k)} - g_{(i-1,j,k)}$$
$$G_y = g_{(i,j+1,k)} - g_{(i,j-1,k)}$$
$$G_z = g_{(i,j,k+1)} - g_{(i,j,k-1)}$$

The components of the surface normals are normalized as:

$$N_u = \frac{G_u}{\sqrt{(G_x)^2 + (G_y)^2 + (G_z)^2}}, \qquad u = x, y, z.$$

The gradients are typically computed either from 6 central neighbors in the $3 \times 3 \times 3$ neighborhood, or from all 26 neighbors. In the latter case the algorithm is identical to the Zucker-Hummel operator for edge detection (Zucker and Hummel 1979). The images in this paper have been computed with 26 neighbors. Using the normal vectors, the object can be shaded according to any shading model, such as Phong shading, which has been used throughout this paper.
Owing to the high dynamic range of the gray levels a continuous shading is now possible that leads to a more realistic impression of the objects. Small details not visible with the Z-buffer gradient shading, such as the suture of a skull, now become recognizable (Fig. 3c). In addition, aliasing effects, which are present in ZG shading, especially during rotation, do not occur. In the case of small objects, however, such as the thin bone in the orbita or the nasal septum, this method leads to artifacts. This is because, in this case, the gray level is no longer governed by the membership to an object class, but by the thickness of the object. As a consequence, the gray-level threshold is not representative for a surface, and the gradient is also not representative for its inclination. It has been claimed (Levoy 1988) that in cases in which exact segmentation is difficult, a semi-transparent modeling of the object could improve the visualization.
In Levoy's algorithm a transparency value is assigned to each voxel depending on its gray level and on its gray-level gradient. In this case too, the shading is done by the gray-level gradient method.

Our preliminary experience with this transparent gray level gradient (TGG) shading method shows that small details on an otherwise compact surface (e.g., bone sutures) can show up very well (see Fig. 3d). However, really problematic regions, such as the orbital cavity or the deformed nasal septum, are not recognized any better, although the image looks smoother. An additional problem with the TGG method is that two parameters can be chosen arbitrarily: the assignment of a transparency to the gray levels and the weight of the gradient. In this manner, a very broad spectrum of visual impressions can be obtained from a single object and it is difficult to decide which are the most accurate.

Since it is obviously difficult to evaluate surface-rendering algorithms without being able to recognize the true surface, we have started a study on the quantification of image quality. Geometrically simulated objects undergo the same data acquisition and processing steps as the real ones. Global and local error measures for the surface location and inclination are computed. Figure 4 shows an error image of the surface normals for an object shaded with Z-buffer gradient or GG shading, respectively. From this image we infer that GG shading involves a much lower error rate, yields smooth surfaces, and even visualizes a slit 0.5 voxels wide. Despite the large numerical errors, the Z-buffer gradient image represents the shape of the object very well. The slit, however, is not recognizable. For further results we refer to Pommert et al. (1989a, b).

2.4 Cut planes

Once a surface view is available, a very simple and effective method of visualizing interior structures is cutting. It is easy to carry out in the ray-casting environment. In our implementation, arbitrary oblique cuts can be specified through three points on the visible surface or on an already existing cut (see Fig. 5). A special case is selective cutting, in which, in the case of multiple objects, surfaces may be excluded from cutting (Fig. 6).

2.5 Transparent visualization

Our experience with 3D visualization of tomographic volumes shows that if exact surfaces can be determined, non-transparent rendering yields the best perception. This is especially true when no additional depth cue, such as motion or binocular stereo, can be used. If exact surface definition by segmentation is not possible, because there is not enough contrast or the objects are too small (as in the case of blood vessels), the only solution is *transparent visualization*. In the case of the visualization of a beating heart from MRI data we used the TGG algorithm on account of segmentation problems. A manual segmentation would not have succeeded since the data set contained 28 slices for each of 12 heart phases. As shown in Fig. 7, the visual impression is fairly good, yet we do not know how precisely it represents the actual surface.

5

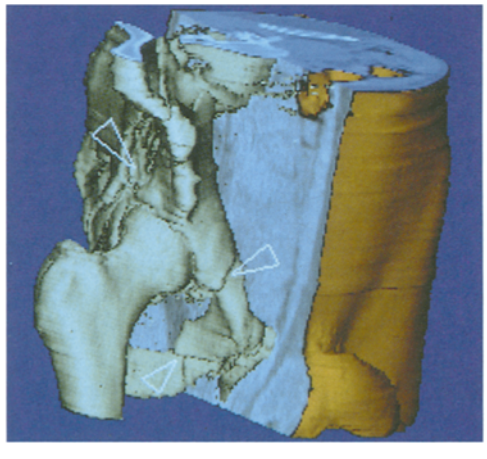

6

Fig. 5. Menu surface of the program VOXEL-MAN with a demonstration of the possibilities of arbitrarily cutting MRI objects

Fig. 6. View of a male pelvis with multiple fractures (*arrows*) from 77 CT slices (bone and skin gray-level gradient shading)

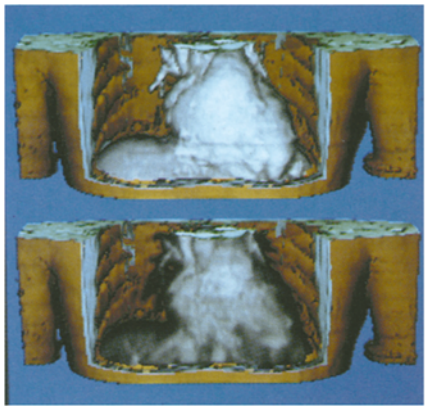

7

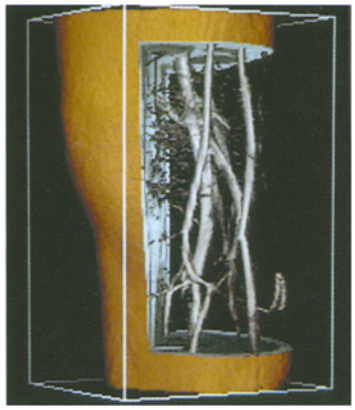

8

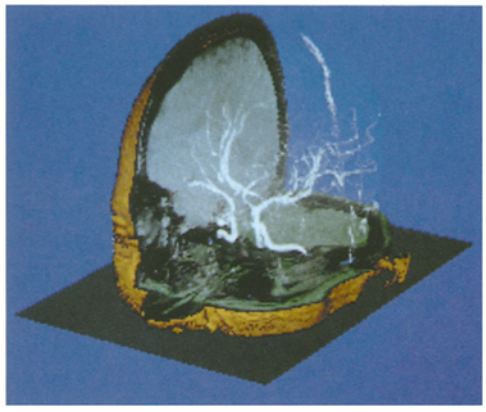

9

Fig. 7. Views of a human heart reconstructed from 28 MRI slices. For the heart itself transparent gray-level gradient shading has been used with low (*upper image*) and high (*lower image*) transparency

Fig. 8. View of a human knee with its blood vessels reconstructed from 64 MRI slices. The vessels are rendered using transparent gray-level gradient shading

Fig. 9. View of a human brain with its blood vessels reconstructed from 118 MRI slices. The vessels are visualized with a transparent maximum intensity projection

A similar problem arises in the case of small vessels. Even if their contrast is good, the neighborhood is not large enough for the determination of a 3D surface. Transparency, however, provides some kind of averaging, leading to a satisfactory visualization, as shown in Fig. 8, in which the vessels have been rendered using the TGG algorithm. If the vessel diameters reach one voxel in width, shading will fail. In this case, visualization of the maximum intensity along the ray has proved to yield surprisingly good results (Fig. 9).

2.6 *Improvement through extended object descriptions*

So far the definition of the objects displayed has been made by thresholding the intensity profile while traversing the volume. A more detailed object definition cannot be achieved through the analysis of the intensity along the ray, since we need a larger 3D neighborhood for the decision of whether a voxel belongs to a surface or not. Another possibility is to gain this information from an additional source. In 2.6.1 and 2.6.2, we describe two methods of extended description, organ labels gained through segmentation and the addition of a second imaging modality.

2.6.1 Segmentation

For the determination of object surfaces other than bone and skin segmentation, algorithms are necessary that take larger voxel neighborhoods into account than is possible in the 1D ray-casting case. In order to find the intensity changes that represent surfaces, we applied a 3D extension of the Marr-Hildreth operator (Marr and Hildreth 1980), which is defined by

$$I'(x, y, z) = \nabla^2 (I(x, y, z) * G(x, y, z, \sigma)),$$

where ∇^2 is the Laplace operator, I the image volume, and G the Gaussian function. The zero crossings of I' are considered as surfaces. By definition these are closed; this is important for 3D display. We have applied this method to MRI data of the head (Bomans et al. 1987, 1989). After binarizing the filtered volume I', the regions obtained are labeled according to their correspondence to different constituents (skin, bone, brain, etc.). In our current procedure this is done interactively for each slice. The regions found do not always correspond to anatomical structures. Errors are corrected by removing wrong connections or by inserting new surface elements. For the segmentation of the brain cortex, for example, we typically correct ten 2D contours. For the 3D contour of the cortex we

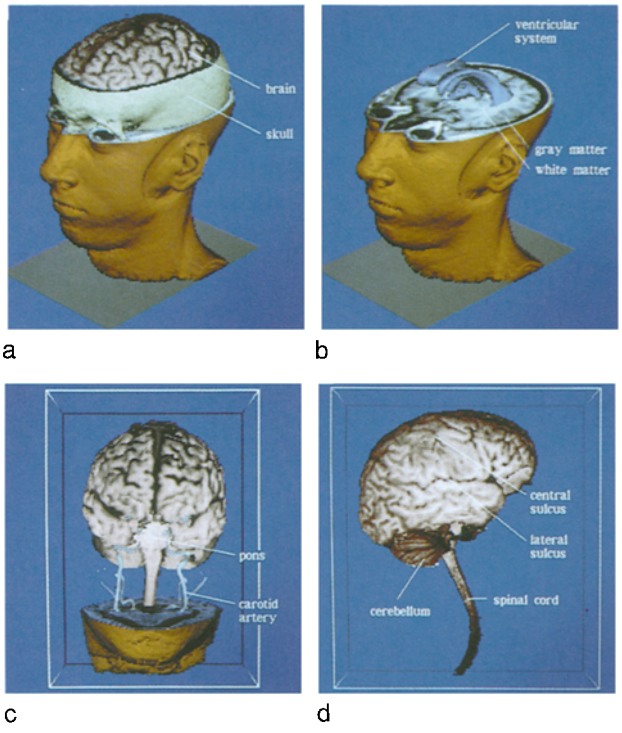

Fig. 10a–d. Views of a human head reconstructed from 128 MRI slices. The surfaces of bone, brain, and ventricular system have been determined by the Marr-Hildreth operator. Shading: skin, bone, and ventricle, gray-level gradient shading; brain and carotid artery, "integral shading"

apply in addition a 3D dilation with a subsequent erosion. This procedure destroys small details of the contour. If, however, we use the 3D contour obtained in this manner as a baseline for a semi-transparent display – here just an integration over 6 pixels ("integral shading") – we obtain images as shown in Fig. 10.

2.6.2 Multiple imaging modalities

A 3D image that is generated from a single imaging modality shows only certain aspects of the actual volume. Improved information can be obtained by combining data of different modalities such as CT, MRI or PET. In this manner bone structures, for example, may be described better by CT, while soft tissue properties are better represented by MRI. Generally, the different data sets do not match geometrically. It is therefore necessary to register the volumes in relation to each other. We have developed a basic tool called a *3D specifier*: corresponding landmarks specified on surface images of MRI

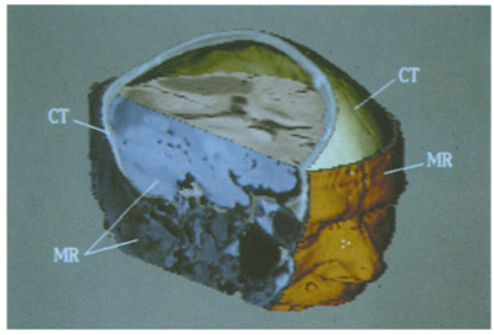

Fig. 11. View of a head of a cadaver with bone taken from CT and tissue from MRI

or CT volumes can be used for the computation of polynomials performing the required 3D distortion (Schiers et al. 1989). Preliminary experience shows that this kind of specification needs a well-trained user and sometimes more than one attempt to arrive at a satisfying match. Figure 11 shows an image obtained using this method, exhibiting the combined properties of MRI and CT.

3 Implementation aspects

The described algorithms are implemented within the program system VOXEL-MAN on a VAX 11/780 (24 Mbytes of main memory) and a VAX station II/GPX (16 Mbytes of main memory). The rotation of a volume of 256^3 voxels takes 15–30 min. The described projections take 10–60 s. Such times are certainly not sufficient for clinical work, but can be tolerated in a research environment. In the meantime, a subset of the algorithms has been implemented on a processor manufactured by the KONTRON Corp. Here a view from any direction shaded with GG shading takes 5–10 s. If we take into account the fast progress in hardware development, computing speed will not be a major issue in the future.

The main problem to be solved to achieve a broad application of the method is the design of an appropriate user interface. Presently VOXEL-MAN has two interfaces: one is a language interface that allows the specification of the desired action using a string of parameters. It has full flexibility, but it needs an expert to choose the right combination from a choice of more than 30 parameters. The other interface is a menu interface that is certainly suitable for the beginner. However, not all specifications can be expressed suitably in this form (see Fig. 5).

4 Applications

3D Imaging, especially of bone, has for several years proved to be useful in craniofacial surgery (Fig. 3), traumatology (Fig. 6), and orthopedics. The possibilities shown in this paper lend themselves to further applications.

In diagnostic radiology the assessment of arbitrary cross sections is facilitated. Although of course radiologists are well accustomed to mentally projecting 3D visualizations from multiple 2D images, these techniques facilitate rapid and sure orientation, particularly in instances where the angle of slice is unusual or unconventional. Once the outer surface and/or bone is visibly defined in three dimensions, the viewer can always be sure about the position of the cross section he is looking at.

It is obvious that neurosurgical therapy will benefit. The relationships between regions to be treated (e.g., tumors) and those which have to be conserved (e.g., blood vessels) can be assessed prior to an operation (Figs. 8, 9). For broader applications, however, the procedures are still too complicated.

The high realism of the images gained from living persons makes them suited for computer-aided teaching in anatomy. Here we can afford the high expenditure of work, because we have to process only a small number of specimens, from which we can make any number of copies. Since the time of Leonardo da Vinci, anatomical instruction material has been painted (Fig. 12). Computer graphics may replace such paintings to a large extent (see Fig. 10).

It is one of the exciting aspects of science that once a principle is discovered it can be applied to various fields that were not necessarily thought of at the beginning. In fact, the pictures in Fig. 12 were generated from a 2600-year-old Egyptian mummy, the interior of which could be explored by our colleagues in the Institute of Anthropology in Tübingen without harming it.

5 Conclusions

We have demonstrated that by using a ray-casting algorithm and the generalized voxel model, natural and detailed 3D images of human anatomy can be obtained. We can draw the following detailed conclusions:

- Surface rendering is decisively improved by using gray-level gradients for the determination of the surface normals.
- Semi-transparent surface rendering is recommended only in cases where the surfaces cannot be determined precisely (e.g., vessels).

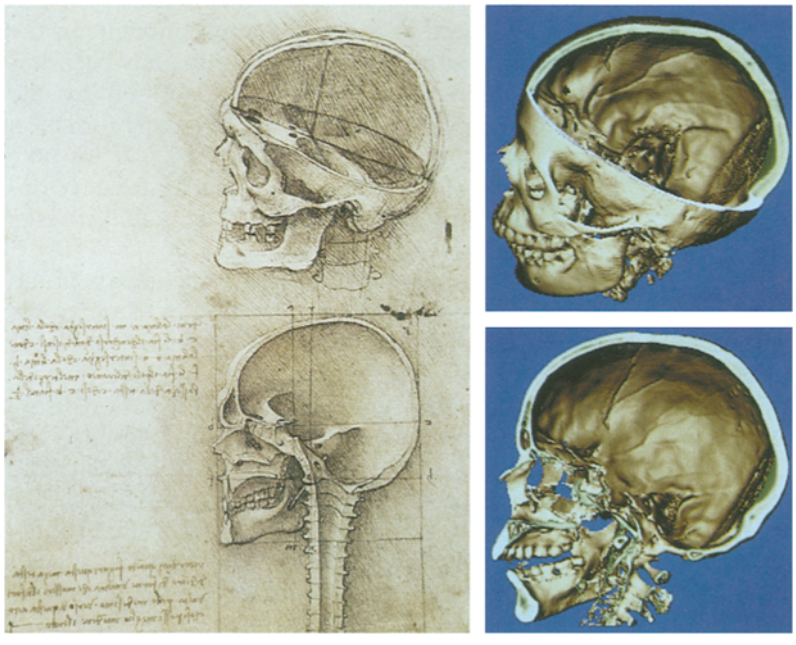

Fig. 12. Leonardo da Vinci's famous drawings of a skull in comparison to analogous aspects of a 2600-year-old Egyptian mummy generated from 200 computer tomograms

- At least in the case of MRI, more detailed object definitions can be achieved by segmentation or multi-modality imaging, thus allowing the display of multiple objects.
- Combining multiple surfaces with different kinds of shading and cuts through the volume allows detailed visualization of tomographic volumes, especially if it can be done interactively.
- As computing power will not be an issue in the future, the problem to be solved is the design of a user interface that will allow easy and consistent specification of the various possible manipulations that we have described.

Acknowledgements. The authors would like to thank Professor Wolf-Joachim Höltje (Department of Craniofacial Surgery), Professor Wolfgang Schulze (Department of Anatomy), Dr. Jürgen Wening (Department of Traumatology), and Dr. Gerd Witte (Department of Radiology) for many discussions. We also thank Ellen Vaske and Rainer Schubert for their help. We are grateful to Siemens (Erlangen) for providing the original MRI volume data from which the perspective views have been produced. The images of the mummy were produced in collaboration with the Institute of Anthropology and the Department of Neuroradiology, University of Tübingen. The tomograms of the cadaver have kindly been provided by the Department of Neuroanatomy, Medical University of Hanover.

References

Barillot C, Gibaud B, Luo LM, Scarabin IM (1985) 3-D Representation of anatomic structures from ct examinations. Biostereometrics '85. Proc SPIE 602:307–314

Boecker FRP, Tiede U, Höhne KH (1985) Combined use of different algorithms for interactive surgical planning. In: Lemke U et al. (eds) Computer assisted radiology. Springer, Berlin Heidelberg New York, pp 572–577

Bomans M, Riemer M, Tiede U, Höhne KH (1987) 3-D Segmentation von Kernspintomogrammen. Ninth DAGM Meeting, Braunschweig. Informatik Fachberichte 149:231–235

Bomans M, Höhne KH, Riemer M, Tiede U (1989) 3D-Segmentation of MR images of the head for 3D-display. IEEE Trans Med Imaging (in press)

Chen LS, Herman GT, Reynolds RA, Udupa JK (1985) Surface shading in the cuberille environment. Comput Graph Appl 5:33–43

Goldwasser SM, Reynolds RA, Bapty T, Baraff D, Summers J, Talton DA, Walsh E (1985) Physicians workstation with real time performance. Comput Graph Appl 5:44–57

Hemmy DC, David DJ, Herman GT (1983) Three-dimensional reconstruction of craniofacial deformity using computed tomography. Neurosurgery 13:534–541

Herman GT, Vose WF, Gomori JM, Gefter WB (1985) Stereoscopic computed three-dimensional surface displays. Radiographics 5:825–852

Höhne KH, Bomans M, Tiede U, Riemer M (1988) Display of multiple 3D-objects using the generalized voxel-model. Proc SPIE 914:850–854

Höhne KH, DeLaPaz RL, Bernstein R, Taylor RC (1987) Combined surface display and reformatting for the 3D analysis of tomographic data. Invest Radiol 22:658–664

Höhne KH, Bernstein R (1986) Shading 3D images from CT using gray level gradients. IEEE Trans Med Imaging 5:45–47

Jackel D (1985) The graphics PARCUM system: a 3D memory based computer architecture for processing and display of solid objects. Computer Graphics Forum 4:21–32

Kaufman A (1986) Voxel based architectures for three-dimensional graphics. Proc IFIP 86:361–366

Lenz R, Danielsson PE, Cronström S, Gudmundson B (1986) Interactive display of 3D medical objects. In: Höhne KH (ed) Pictorial information systems in medicine. Springer, Berlin Heidelberg New York, pp 449–468

Levoy M (1988) Display of surface from volume data. IEEE Comput Graph and Appl 8:29–37

Lorensen WE, Cline HE (1987) Marching cubes: A high resolution 3D surface construction algorithm. Computer Graphics 21:163–169

Marr D, Hildreth EC (1980) Theory of edge detection. Proc R Soc Lond [B] 207:187–217

Pommert A, Bomans M, Tiede U, Höhne KH (1989a) Image Quality in voxel-based Surface shading. In: Lemke HU et al (eds) Computer assisted radiology (Proc CAR '89). Springer, Berlin Heidelberg New York 737–741

Pommert A, Bomans M, Tiede U, Höhne KH (1989b) Simulation studies for quality assurance of 3D-images from computed tomograms. In: Todd-Pokropek A, Viergever MA (eds) The formation, handling and evaluation of medical images. (NATO ASI Series F, Computer and Systems Sciences) Springer, Berlin Heidelberg New York (in press)

Schiers C, Tiede U, Höhne KH (1989) Interactive 3D registration of image volumes from different sources. In: Lemke HU et al. (eds), Computer assisted radiology. (Proc. CAR '89) Springer, Berlin Heidelberg New York, pp 666–670

Templeton AW, Johnson JA, Anderson WH (1985) Computer graphics for digitally formatted images. Radiology 152:527–528

Tiede U, Höhne KH, Riemer M (1987) Comparison of surface rendering techniques for 3D tomographic objects. In: Lemke U et al. (ed) Computer assisted radiology. Springer, Berlin Heidelberg New York, pp 599–610

Tiede U, Riemer M, Bomans M, Höhne KH (1988) Display techniques for 3D-tomographic volume data. In Proc. NCGA '88, vol III. Anaheim, pp 188–197

Vannier MW, Marsh JL, Warren J (1984) Three-dimensional CT reconstruction images for craniofacial surgical planning. Radiology 150:179–184

Witte G, Höltje W, Tiede U, Riemer M (1986) Die dreidimensionale Darstellung computertomographischer Untersuchungen kraniofacialer Anomalien. Fortschr Röntgenstr 144:24–29

Yasuda T, Toriwaki J, Yokoi S, Katada K (1984) Three-dimensional display system of CT images for surgical planning. International Symposium on Medical Images and Icons, Silver Spring Md. IEEE Computer Society, pp 322–327

Zucker SW, Hummel RA (1979) An optimal three-dimensional edge operator. McGill Univ Rep 79–10

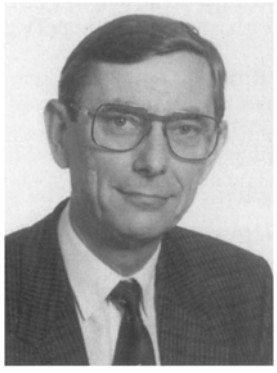

KARL HEINZ HÖHNE is a professor of medical informatics and director of the Department of Computer Science in Medicine at the University of Hamburg. His current research interests include techniques for the visualization and management of pictorial information for medical diagnosis, treatment, and education.
Höhne received his MS in physics from the University of Würzburg and his Ph.D. from the University of Hamburg, Germany.

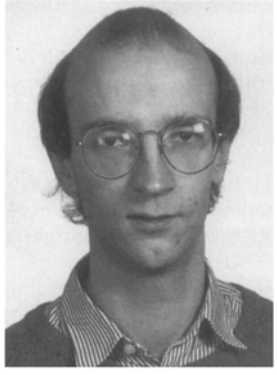

MICHAEL BOMANS is a research assistant at the Department of Computer Science in Medicine, University of Hamburg. He is working on image processing and computer graphics and his special research interests are 3D edge detection and segmentation of tomographic volumes.
Bomans studied computer science at the University of Hamburg and received his M.S. in Computer Science in 1986.

ANDREAS POMMERT is a research assistant at the Department of Computer Science in Medicine, University of Hamburg, where he is engaged in medical image processing and computer graphics. His primary research interests are in quality assurance for 3D display techniques. He is responsible for the research communication system installed at the University Hospital Eppendorf.
Pommert has worked on several software projects in West Germany and the USA. He received his M.S. in Computer Science at the University of Kiel in 1987.

MARTIN RIEMER is a staff member of the Institute of Mathematics and Computer Science in Medicine. He is in charge of the system programming and software engineering of the department's imaging computer facilities. His main interests are image processing and computer graphics of 3D and 4D data.
Riemer received his M.S.E.E. degree from the Fachhochschule Wedel, FRG in 1976.

CARSTEN SCHIERS has been working at the Department of Computer Science in Medicine, University of Hamburg, since 1986. His research interests include medical applications of computer science and in particular computer vision. He is a graduate student in computer science. Presently he is preparing his M.S. thesis on 3D registration of medical image volumes.

ULF TIEDE is a research assistant at the Institute of Mathematics and Computer Science in Medicine at the University Hospital Eppendorf, Hamburg. He is working on image processing, computer graphics algorithms and user interface design for 3D medical workstations. His research interest includes display techniques for voxel-based data and simulation of surgical therapy planning. Tiede received his M.S. in Computer Science at the University of Hamburg in 1988.

GUNNAR WIEBECKE has been working at the Department of Computer Science in Medicine, University of Hamburg, since 1986. His research interests include medical applications of computer science and in particular computer vision. He is a graduate student in computer science. Presently he is preparing his M.S. thesis on the visualization of 3D objects without explicit segmentation.